Electronic Supplementary Material (ESI) for Physical Chemistry Chemical Physics.

Effects of solvent molecules on hemi-bonded $(CH_3SH)_2^+$: infrared absorption of $[(CH_3SH)_2\text{-}X]^+$ with X = H_2O, $(CH_3)_2CO$, or NH_3 and $(CH_3SH)_n^+$ (n = 3−6)

Min Xie,[*ab] Huei-Ru, Tsai,[a] Asuka Fujii,[c] and Yuan-Pern Lee[*ade]

[a]*Department of Applied Chemistry and Institute of Molecular Science, National Chiao Tung University, 1001, Ta-Hsueh Road, Hsinchu 30010, Taiwan*

[b]*MOE Key Laboratory of Laser Life Science & Institute of Laser Life Science, College of Biophotonics, Guangzhou Key Laboratory of Spectral Analysis and Functional Probes, South China Normal University, Guangzhou 510631, China*

[d]*Department of Chemistry, Graduate School of Science, Tohoku University, Sendai 980-8578, Japan*

[d]*Center for Emergent Functional Matter Science, National Chiao Tung University, Hsinchu 30010, Taiwan*

[e]*Institute of Atomic and Molecular Sciences, Academia Sinica, Taipei 10617, Taiwan*

*E-mail: xiemin@m.scnu.edu.cn (MX); yplee@mail.nctu.edu.tw (YPL)

Table of Contents

Table S1 Comparison of predicted scaled harmonic vibrational wavenumbers and IR intensities of $[(CH_3SH)_2\text{-}H_2O]^+$ with experiments.

Table S2 Comparison of predicted scaled harmonic vibrational wavenumbers and IR intensities of $[(CH_3SH)_2\text{-}(CH_3)_2CO]^+$ with experiments.

Table S3 Comparison of predicted scaled harmonic vibrational wavenumbers and IR intensities of $[(CH_3SH)_2\text{-}NH_3]^+$ with experiments.

Table S4 Comparison of predicted scaled harmonic vibrational wavenumbers and IR intensities of $(CH_3SH)_3^+$ with experiments.

Table S5 Second-order perturbation energy $E(2)$ (kJ mol^{-1}) for the intermolecular interactions in $[(CH_3SH)_2\text{-}X]^+$ with X = H_2O or CH_3SH or $(CH_3)_2CO$ or NH_3, predicted at the UB3LYP/aug-cc-pVDZ method with the structures optimized at UMP2/aug-cc-pVDZ method.

Fig. S1 Representative geometric parameters of six structures of $[(CH_3SH)_2\text{-}H_2O]^+$ predicted with the UMP2/aug-cc-pVDZ method.

Fig. S2 Representative geometric parameters of six structures of $[(CH_3SH)_2\text{-}(CH_3)_2CO]^+$ predicted with the UMP2/aug-cc-pVDZ method.

Fig. S3 Representative geometric parameters of five structures of $[(CH_3SH)_2\text{-}NH_3]^+$ predicted with the UMP2/aug-cc-pVDZ method.

Fig. S4 Representative geometric parameters of three structures of $(CH_3SH)_3^+$ predicted with the UMP2/aug-cc-pVDZ method.

Fig. S5 Comparison of observed spectrum of $(CH_3SH)_4^+$ with the stick spectra of possible structures predicted with the UMP2/aug-cc-pVDZ method in region 2000−3150 cm^{-1}.

Fig. S6 Comparison of observed spectrum of $(CH_3SH)_5^+$ with the stick spectra of possible structures predicted with the UMP2/aug-cc-pVDZ method in region 2000−3200 cm^{-1}.

Fig. S7 Comparison of observed spectrum of $(CH_3SH)_6^+$ with the stick spectra of possible structures predicted with the UMP2/aug-cc-pVDZ method in region 2000−3200 cm^{-1}.

Table S1 Comparison of predicted scaled harmonic vibrational wavenumbers and IR intensities of $[(CH_3SH)_2\text{-}H_2O]^+$ with experiments.

Experiment	Calculation						Assignment
	$2M_b$-W	**$2M_a$-W**	**M-W-M**	**M-M-W**	**M-MW**	**MW-M**	
3712	3669[a] (116)[b]	3673[a] (115)[b]	3540[a] (194)[b]	3682[a] (134)[b]	3674[a] (118)[b]	3576[a] (206)[b]	*a*-OH-stretch
3629	3561 (54)	3562 (50)		3568 (56)	3559 (51)	3097 (1506)	*s*-OH-stretch
	3054 (0.5)	3055 (8.1)	3061 (0.2)	3069 (2.2)	3060 (6.4)	3059 (5.9)	*a*-CH-stretch
3020	3053 (1.6)	3052 (0.8)	3052 (0.4)	3061 (3.4)	3053 (0.5)	3057 (2.5)	
	3046 (3.3)	3047 (2.5)	3050 (1.1)	3032 (4.0)	3045 (0.6)	3048 (0.5)	
	3045 (0.9)	3042 (4.4)	3005 (3.3)	2998 (4.5)	3016 (4.0)	3034 (12)	
2946	2935 (12)	2934 (6.9)	2945 (2.1)	2946 (0.4)	2938 (3.6)	2941 (5.1)	s-CH-stretch
	2935 (0.1)	2933 (2.1)	2906 (1.5)	2905 (2.5)	2913 (4.4)	2924 (5.2)	
2567	2509 (0.9)	2584 (25)	2601 (4.9)	2599 (7.1)	2615 (5.6)	2615 (5.6)	free SH-stretch
broad feature	2528 (256)	2418 (397)	2229 (1458)[c]	2211 (1128)	1675 (3085)	2584 (30)	H-bonded
			1966 (6554)[c]	1785 (3120)			SH-stretch
	1593 (71)	1589 (66)	1556 (116)	1573 (27)	1575 (150)	1561 (11)	HOH-bend

[a] Calculated with the UMP2/aug-cc-pVDZ method and scaled by a linear equation $y = 0.930\ x + 61.0$, in which x is the harmonic vibrational wavenumber. [b] IR intensities in km mol^{-1}. [c] stretch vibration of H_3O^+. In the structure of **M-W-M** the proton of one CH_3SH transfers to H_2O.

Table S2 Comparison of predicted scaled harmonic vibrational wavenumbers and IR intensities of $[(CH_3SH)_2\text{-}(CH_3)_2CO]^+$ with experiments.

Experiment	Calculation						Assignments
	2M$_b$A	**2M$_a$A**	**M-M-A1**	**M-M-A2**	**M-MA**	**MA-M**	
3020	3050[a] (1.0)[b]	3058[a] (8.9)[b]	3052[a] (0.4)[b]	3061[a] (0.8)[b]	3059[a] (2.8)[b]	3052[a] (0.4)[b]	*a*-CH-stretch
	3050 (1.1)	3049 (0.4)	3050 (3.1)	3059 (1.8)	3053 (0.4)	3052 (1.1)	
	3042 (1.4)	3046 (1.2)	3044 (1.1)	3028 (1.7)	3047 (0.7)	3044 (2.5)	
	3042 (0.4)	3042 (3.1)	2990 (4.4)	2993 (2.1)	3030 (6.0)	3044 (5.2)	
	3039 (1.1)	3037 (3.5)	3054 (2.2)	3047 (1.9)	3048 (1.2)	3038 (1.7)	*a*-CH-stretch
	3038 (11)	3031 (8.4)	3052 (0.5)	3034 (6.8)	3044 (3.4)	3001 (0.6)	of $(CH_3)_2CO$
	2996 (0.1)	2996 (0.5)	2999 (1.5)	2997 (0.5)	2998 (0.6)	2997 (0.3)	
	2990 (0.0)	2990 (0.1)	2989 (1.3)	2990 (0.1)	2992 (0.5)	3018 (31)	
2946	2932 (10)	2934 (4.2)	2940 (6.8)	2943 (0.6)	2941 (5.5)	2941 (8.8)	*s*-CH-stretch
	2932 (0.4)	2930 (2.0)	2903 (4.7)	2900 (0.1)	2925 (0.9)	2908 (26)	
	2917 (0.7)	2915 (0.9)	2912 (11)	2917 (2.5)	2917 (1.7)	2913 (2.2)	*s*-CH-stretch
	2912 (0.3)	2911 (0.4)	2902 (13)	2912 (1.9)	2912 (2.2)	2910 (2.7)	of $(CH_3)_2CO$
2559	2443 (16)	2582 (22)	2615 (2.5)		2605 (1.8)	2616 (1.6)	free SH-stretch
						2593 (25)	
broad feature	2472 (662)	2253 (1041)	2364 (3432)	1941 (2049)	1981 (2072)		H-bonded SH-stretch
				1697 (586)			

[a] Calculated with the UMP2/aug-cc-pVDZ method and scaled by a linear equation $y = 0.930\ x + 61.0$, in which x is the harmonic vibrational wavenumber. [b] IR intensities in km mol^{-1}.

Table S3 Comparison of predicted scaled harmonic vibrational wavenumbers and IR intensities of $[(CH_3SH)_2\text{-}NH_3]^+$ with experiments.

Experiment	Calculation					Assignments
	M-M-N	**2M$_b$N**	**2M$_a$N**	**M-MN**	**MN-M**	
3379	3387[a] (104)[b]	3383[a] (96)[b]	3383[a] (99)[b]	3429[a] (58)[b]	3433[a] (60)[b]	*a*-NHx-stretch
		3380 (107)	3380 (108)	3424 (65)	3358 (195)	
3320	3314 (179)	3258 (90)	3258 (100)	3267 (73)	3143 (488)	*s*-NHx-stretch
	3050 (1.1)	3056 (2.6)	3049 (3.2)	3051 (0.4)	3056 (4.6)	
	3044 (0.8)	3046 (0.8)	3045 (0.2)	3050 (1.3)	3055 (0.3)	*a*-CH-stretch
	3041 (1.2)	3026 (1.6)	3026 (2.3)	3042 (1.1)	3046 (0.8)	
	3004 (4.5)	3008 (3.0)	3010 (2.6)	3032 (5.1)	3044 (7.9)	
	2937 (23)	2939 (3.2)	2935 (6.8)	2937 (5.0)	2941 (6.5)	*s*-CH-stretch
	2907 (7.4)	2914 (6.0)	2916 (10)	2928 (2.6)	2933 (2.4)	
broad feature	2917 (1126)	2171 (3408)	2607 (3825)	2127 (1525)		H-bonded NH-stretch
	2781 (1509)					
	2606 (7.8)	2607 (7.3)	2161 (9.7)	2606 (4.9)	2616 (3.4)	free SH-stretch
					2590 (14)	

[a] Calculated with the UMP2/aug-cc-pVDZ method and scaled by a linear equation $y = 0.930\ x + 61.0$, in which x is the harmonic vibrational wavenumber. [b] IR intensities in km mol^{-1}.

Table S4 Comparison of predicted scaled harmonic vibrational wavenumbers and IR intensities of $(CH_3SH)_3^+$ with experiments.

Experiment	Calculation			Assignments
	3M$_a$	**3M$_b$**	**3M$_{HB}$**	
	3051[a] (3.2)[b]	3053[a] (0.3)[b]	3060[a] (1.7)[b]	*a*-CH-stretch
	3050 (0.1)	3053 (1.3)	3057 (2.5)	
3024	3047 (0.8)	3049 (1.6)	3052 (0.3)	
	3046 (2.8)	3047 (2.7)	3044 (0.8)	
	3040 (1.5)	3045 (1.0)	3030 (5.0)	
	3036 (4.2)	3039 (3.1)	2996 (3.7)	
	2937 (6.0)	2940 (5.3)	2941 (0.2)	*s*-CH-stretch
2947	2932 (6.1)	2935 (7.4)	2938 (4.1)	
	2929 (3.4)	2931 (3.7)	2905 (2.3)	
2595	2608 (4.8)	2610 (3.5)	2600 (4.5)	free SH-stretch of third CH_3SH
2565	2581 (24)	2555 (45)		free SH-stretch
broad feature	2237 (953)	2250 (957)	1884 (1986)	H-bonded SH-stretch
			1660 (4322)	

[a] Calculated with the UMP2/aug-cc-pVDZ method and scaled by a linear equation $y = 0.930\ x + 61.0$, in which x is the harmonic vibrational wavenumber. [b] IR intensities in km mol^{-1}.

.

Table S5 Second-order perturbation energy $E(2)$ (kJ mol^{-1}) for the intermolecular interactions in $[(CH_3SH)_2\text{-}X]^+$ with X = H_2O or CH_3SH or $(CH_3)_2CO$ or NH_3, predicted at the UB3LYP/aug-cc-pVDZ method with the structures optimized at UMP2/aug-cc-pVDZ method.

	Structure	Lp (X) → σ* (SH)	Lp (S) → σ* (XH)
$[(CH_3SH)_2\text{-}H_2O]^+$	**$2M_b$-W**	28.6[a]	--
	$2M_a$-W	30.5	--
$(CH_3SH)_3^+$	**$3M_b$**	43.6	--
	$3M_a$	48.2	--
$[(CH_3SH)_2\text{-}(CH_3)_2CO]^+$	**$2M_b$-A**	42.2	--
	$2M_a$-A	42.0	--
$[(CH_3SH)_2\text{-}NH_3]^+$ [b]	**$2M_b$-N**	--	125.3
	$2M_a$-N	--	125.6

[a] In **$2M_b$-W** and **$2M_b$-A**, the solvent molecule is hydrogen bonded to the two SH bonds in the ion core. [b] the proton was transferred only in the $[(CH_3SH)_2\text{-}NH_3]^+$ cluster, reflecting the interaction of Lp (S) → σ* (XH). The $E(2)$ were predicted at the UB3LYP/aug-cc-pVDZ method with the structures optimized with the UMP2/aug-cc-pVDZ method.

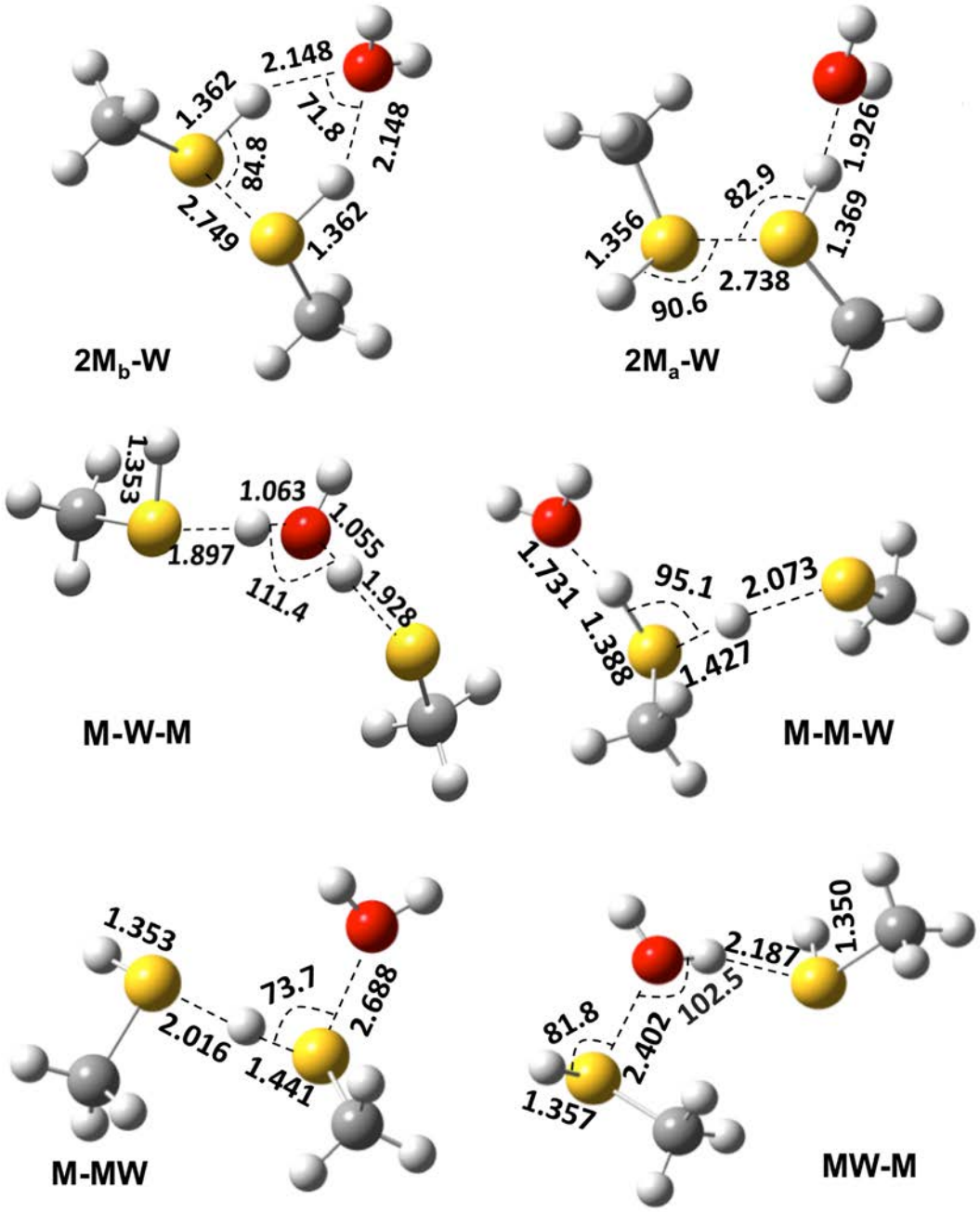

Fig. S1 Representative geometric parameters of six structures of $[(CH_3SH)_2\text{-}H_2O]^+$ predicted with the UMP2/aug-cc-pVDZ method. Bond distances are in Å; bond angles are in degree.

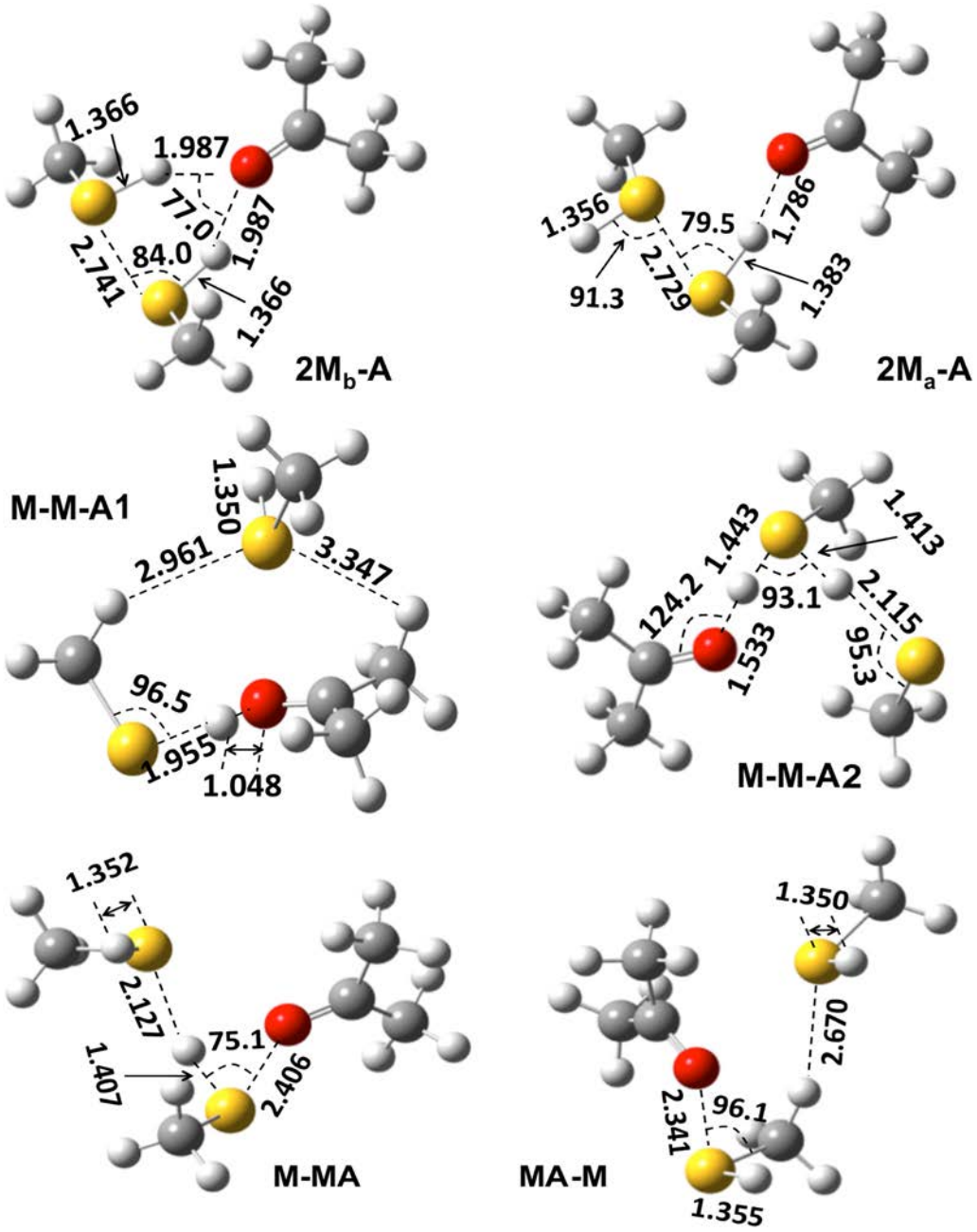

Fig. S2 Representative geometric parameters of six structures of $[(CH_3SH)_2\text{-}(CH_3)_2CO]^+$ predicted with the UMP2/aug-cc-pVDZ method. Bond distances are in Å; bond angles are in degree.

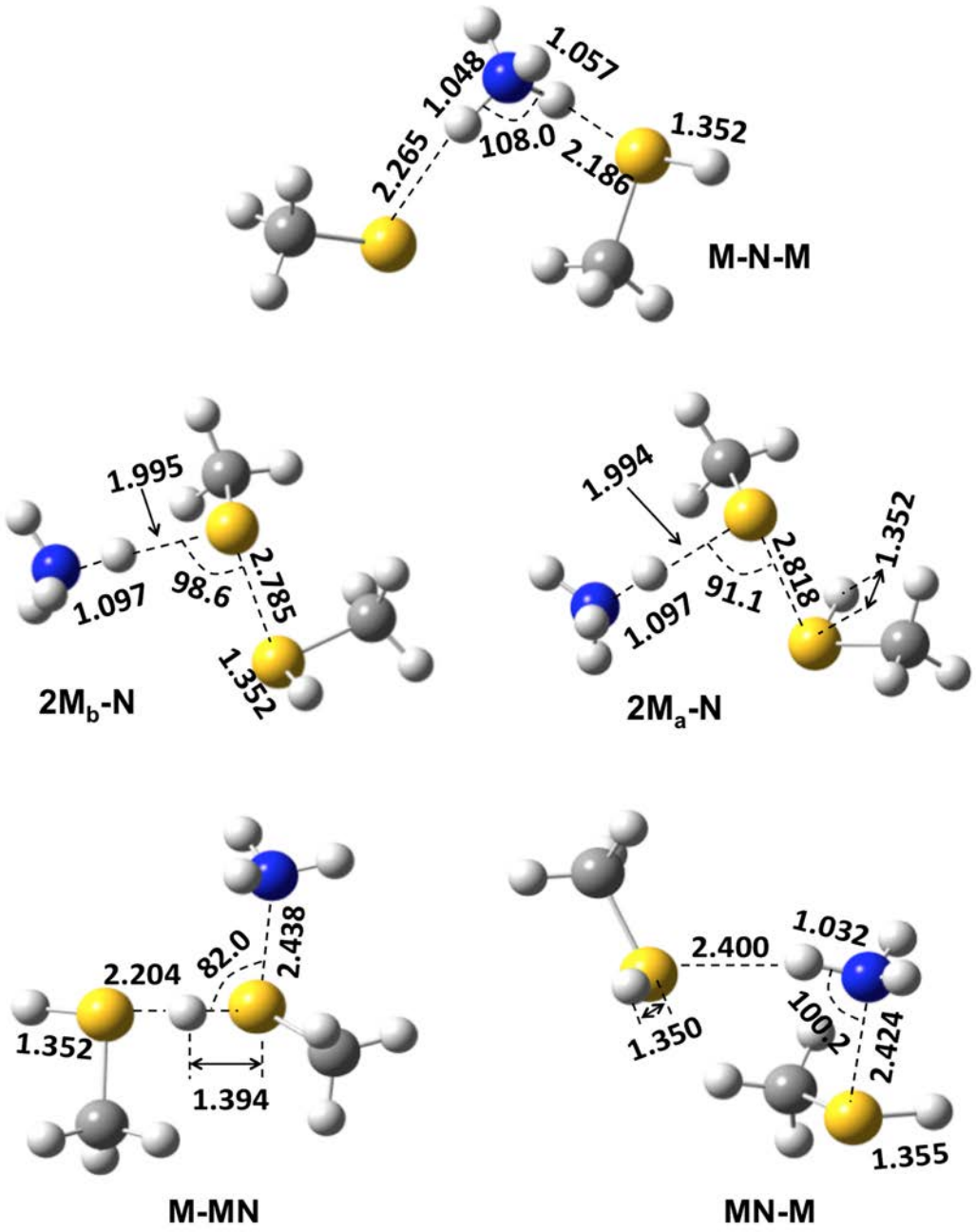

Fig. S3 Representative geometric parameters of five structures of $[(CH_3SH)_2\text{-}NH_3]^+$ predicted with the UMP2/aug-cc-pVDZ method. Bond distances are in Å; bond angles are in degree.

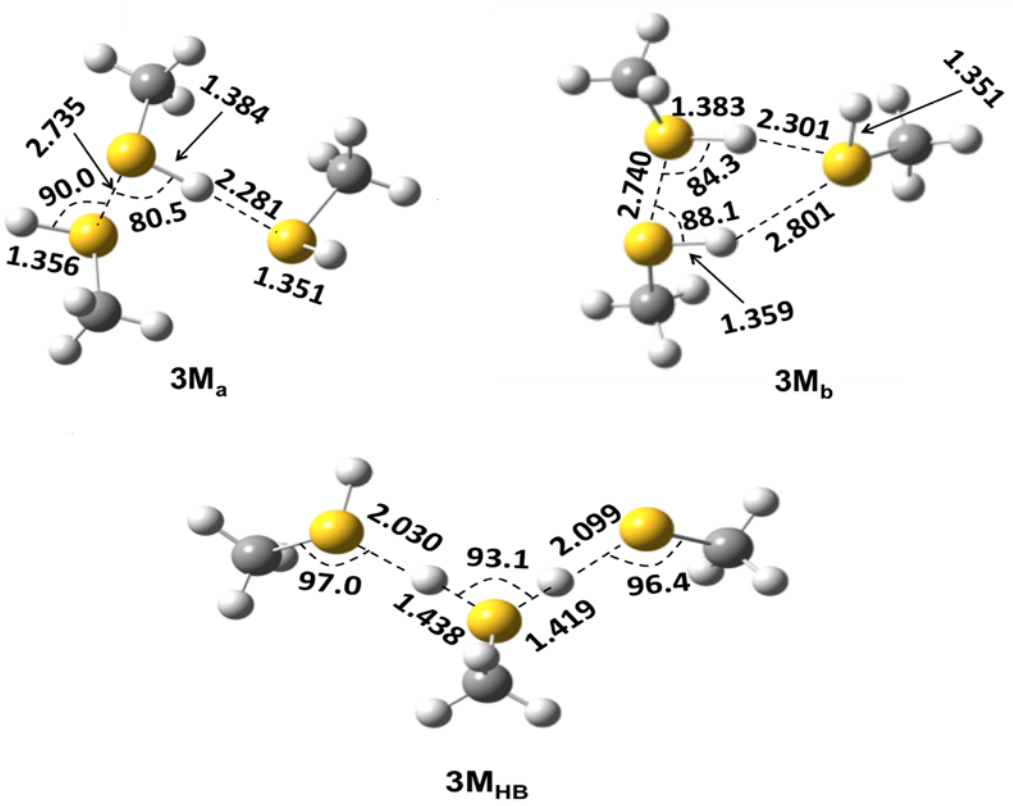

Fig. S4 Representative geometric parameters of three structures of $(CH_3SH)_3^+$ predicted with the UMP2/aug-cc-pVDZ method. Bond distances are in Å; bond angles are in degree.

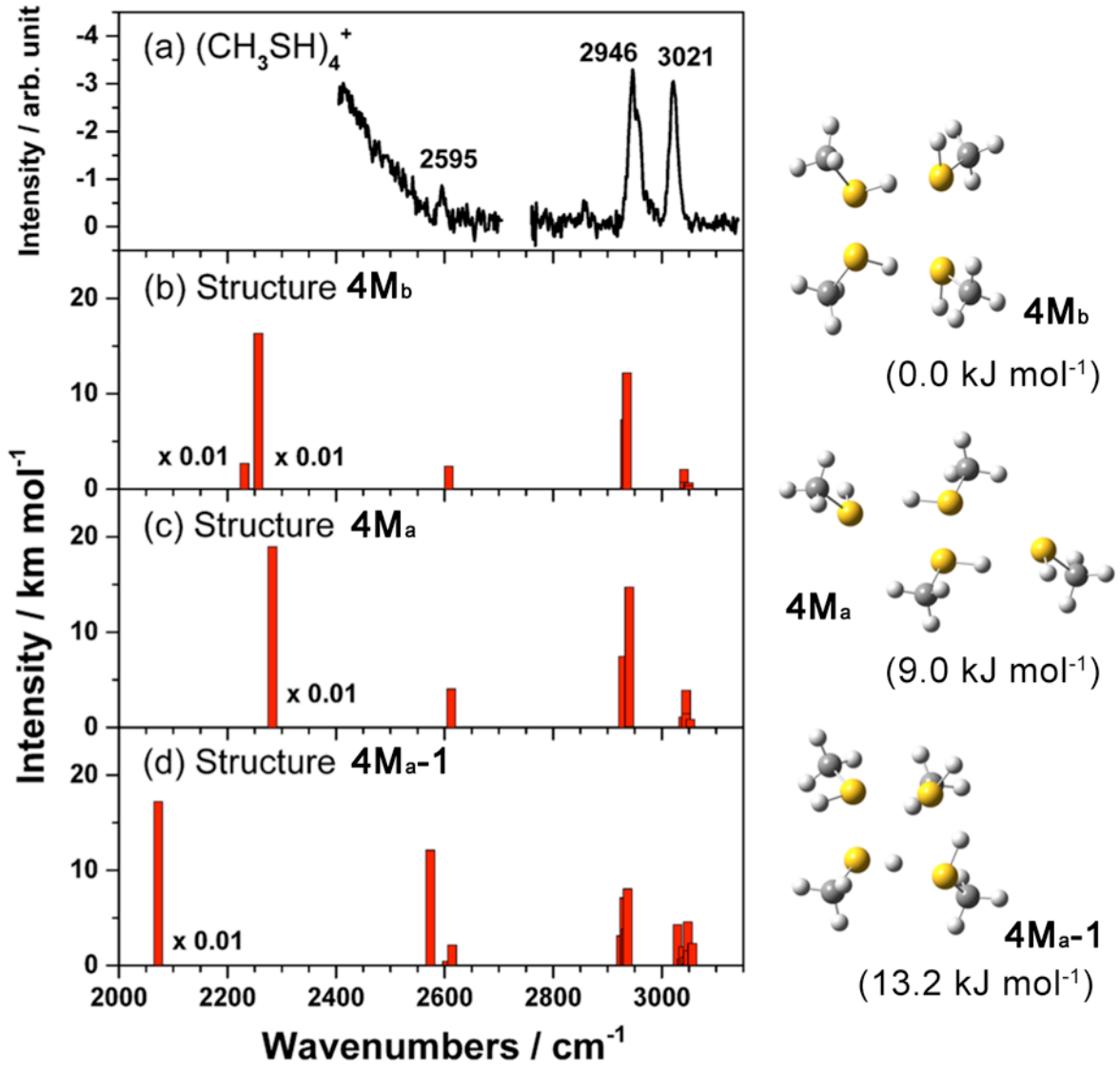

Fig. S5 Comparison of observed spectrum of $(CH_3SH)_4^+$ with the stick spectra of possible structures predicted with the UMP2/aug-cc-pVDZ method in region 2000−3150 cm^{-1}. (a) Experiment; (b) **4M$_b$**; (c) **4M$_a$**; (d) **4M$_a$-1**. The three stable structures are shown on the right with their related energy (kJ mol^{-1}) listed in parenthesis.

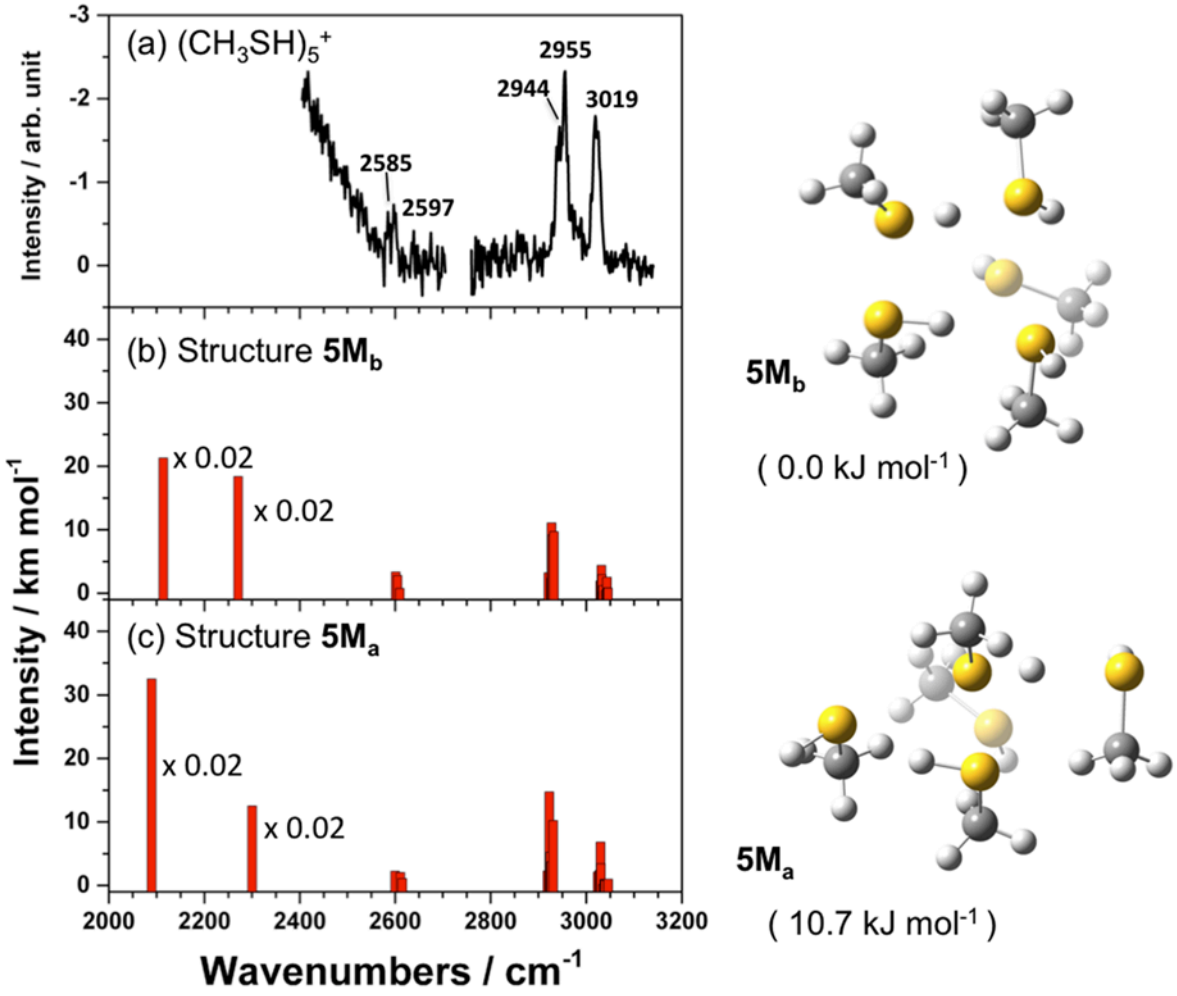

Fig. S6 Comparison of observed spectrum of $(CH_3SH)_5^+$ with the stick spectra of possible structures predicted with the UMP2/aug-cc-pVDZ method in region 2000−3200 cm^{-1}. (a) Experiment; (b) $\mathbf{5M_b}$; (c) $\mathbf{5M_a}$. The two structures are shown on the right with their related energy (kJ mol^{-1}) listed in parenthesis.

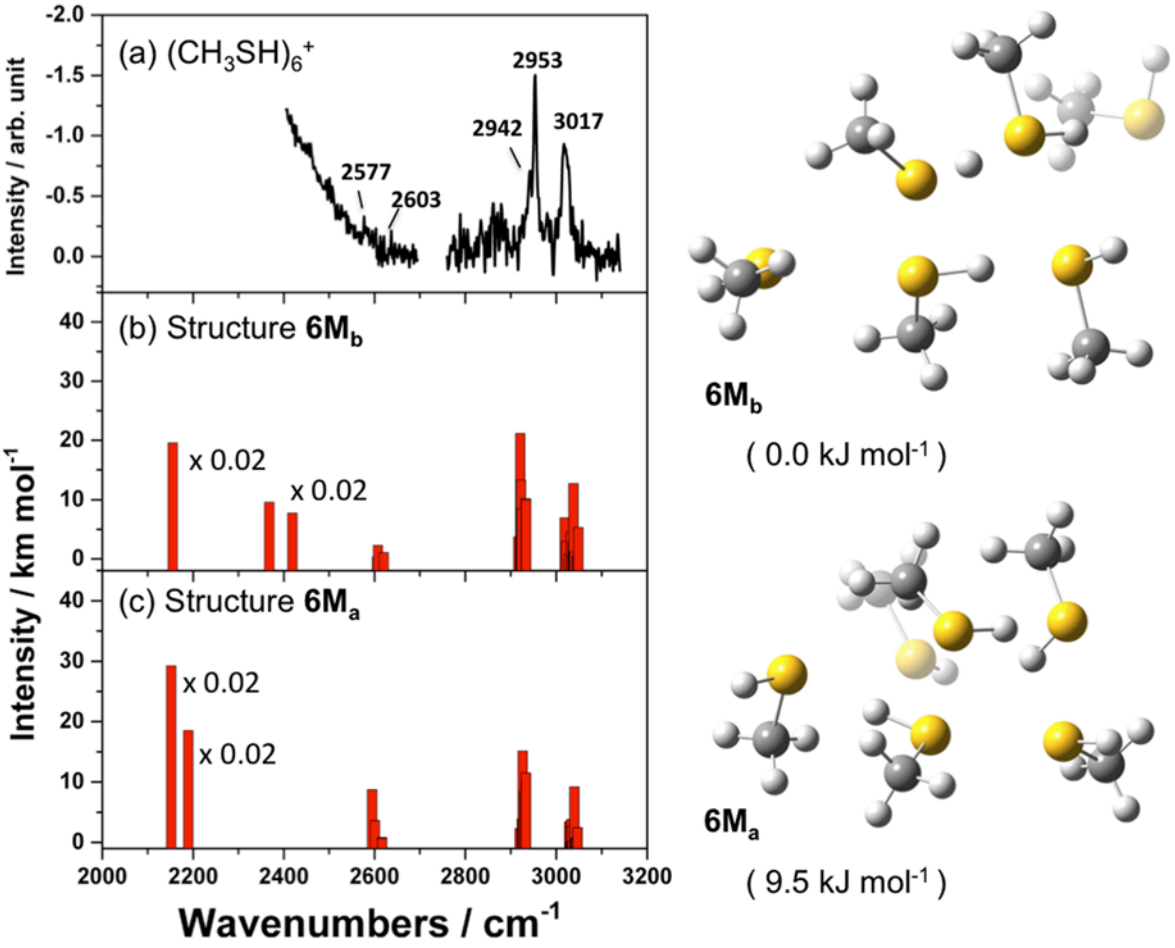

Fig. S7 Comparison of observed spectrum of $(CH_3SH)_6^+$ with the stick spectra of possible structures predicted with the UMP2/aug-cc-pVDZ method in region 2000−3200 cm^{-1}. (a) Experiment; (b) **6M$_b$**; (c) **6M$_a$**. The two structures are shown on the right with their related energy (kJ mol^{-1}) listed in parenthesis.